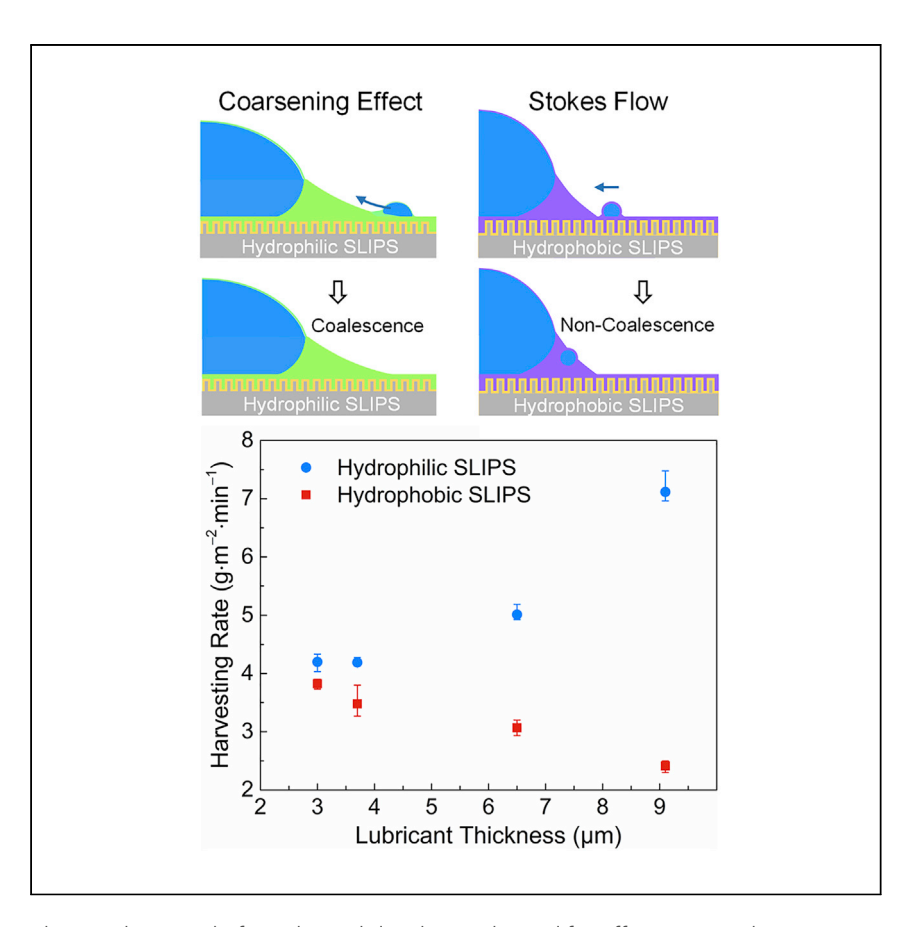




Article

Hydrophilic slippery surface enabled coarsening effect for rapid water harvesting



The rapid removal of condensed droplets is desired for efficient water harvesting. In this work, Guo et al. report a coarsening effect—in other words, smaller droplets climb spontaneously on the oil meniscus of a larger one. This coarsening effect can rapidly remove microscale condensates to increase the water harvesting rate.

Zongqi Guo, Lei Zhang, Deepak Monga, Howard A. Stone, Xianming Dai

dai@utdallas.edu

HIGHLIGHTS

Coarsening effect: meniscusmediated droplet climbing on hydrophilic SLIPS

Microscale water droplets move toward larger ones spontaneously

A thicker hydrophilic lubricant layer shows a higher heat transfer coefficient

A stronger coarsening effect leads to a larger water harvesting rate

Guo et al., Cell Reports Physical Science 2, 100387

April 21, 2021 © 2021 The Author(s). https://doi.org/10.1016/j.xcrp.2021.100387



Article

Hydrophilic slippery surface enabled coarsening effect for rapid water harvesting

Zongqi Guo,¹ Lei Zhang,¹ Deepak Monga,¹ Howard A. Stone,² and Xianming Dai^{1,3,*}

SUMMARY

Water harvesting through the condensation of vapor in air has the potential to alleviate water scarcity in arid regions around the globe. When water vapor is condensed on a cooled surface, tiny water droplets act as thermal barriers. Thus, they must be removed rapidly for efficient water harvesting. Passive technologies for droplet removal rely on in-site growth and direct contact of densely distributed droplets. However, it is challenging to remove submicrometer droplets that lead to a poor water harvesting rate. Here, we present a coarsening effect to rapidly remove water droplets with diameters <20 μm from the hydrophilic slippery liquid-infused porous surface (SLIPS). We quantitatively study the driving and drag forces to enhance the rapid droplet size evolution. The self-propelled coarsening effect enables rapid droplet removal regardless of surface orientations, showing a promising approach compared to those on PEGylated hydrophilic surface, hydrophobic SLIPS, and superhydrophobic surface in water harvesting.

INTRODUCTION

Surfaces that enable rapid vapor-to-liquid condensation and promote droplet removal to reduce thermal resistances are strongly desired for condensation-driven water harvesting. ^{1–5} A hydrophilic surface favors vapor-to-liquid nucleation in a steam environment, but typically the condensed water droplets are pinned on the surface and lead to complete coverage of the surface by a layer of water (i.e., filmwise condensation), which is characterized by a small heat transfer coefficient (HTC) due to the low thermal conductivity of water (0.6 W/m • K at 20°C). ⁶ Liquid-repellent surfaces, either air-infused surfaces (also called superhydrophobic surfaces [SHSs]) or liquid-infused surfaces (also called slippery liquid-infused porous surface), promote dropwise condensation that shows a 10 times higher HTC than filmwise condensation due to the rapid removal of condensates. ⁷

The jumping droplet phenomenon gives rise to a special dropwise condensation. When condensed droplets grow to a certain size, they will coalesce with one another. During the coalescence process of those droplets, their surface energy will be converted to kinetic energy and the coalesced droplets will jump off the surface, which has been shown to produce the effective removal of condensates from the surface. However, the jumping process relies on an air lubricant and hydrophobic coatings, which implies some challenges to effective condensation: (1) air has a much lower thermal conductivity (0.026 W/m • K) than water; (2) hydrophobic surface chemistry hinders vapor-to-liquid nucleation in a steam environment; (3) condensation may occur inside the rough structures, and the condensate can cover the surface; (4) the direct contact of condensed droplets with one another is essential for coalescence, which results in densely distributed droplets and a reduced water-free area for further vapor condensation.

¹Department of Mechanical Engineering, The University of Texas at Dallas, Richardson, TX 75080. USA

²Department of Mechanical and Aerospace Engineering, Princeton University, Princeton, NJ 08544, USA

³Lead contact

^{*}Correspondence: dai@utdallas.edu https://doi.org/10.1016/j.xcrp.2021.100387



Cell Reports
Physical Science
Article

To circumvent the use of an air lubricant, researchers developed the slippery liquid-infused porous surface (SLIPS) by replacing the air lubricant with liquid lubricant. ^{10–12} The original liquid-infused surfaces were designed to minimize the pinning forces and achieve super-liquid repellency, so the surface design did not consider the nucleation process. Liquid-infused surfaces were modified for condensation applications by minimizing the wrapping layer (also called cloaking) ¹³ or creating patterned hydrophilic micropillars to improve nucleation. ¹⁴ Unlike an air lubricant that does not favor thermal conductance, the liquid lubricant completely covers the solid gaps, so the condensation occurs on either the solid or the liquid surface. ¹⁵ When condensed droplets grow to a certain diameter, they are shed from a vertical surface by gravity owing to the small pinning force. ¹³

Recent studies have observed the dynamic movements of water droplets on hydrophobic liquid-infused surfaces. The droplet motion could be controlled by the capillary mechanism similar to the "Cheerios effect" on silicone oil-infused surfaces. 16 Droplets moved to the sidewalls of the channel through the oil meniscus at the sharp corners.¹⁷ Likewise, the silicone oil menisci formed around patterned hydrogel dots could generate a contact angle gradient on the two sides of each droplet so that all of the surrounding droplets move toward the hydrogel dots. 18 By adding hollow channels in the center of the patterned hydrogel dots, directional water droplet pumping and collection were achieved. 19 On Krytox oil-infused surfaces, condensed smaller droplets could also move toward larger ones, but the speed decreased sharply as the smaller droplet entered into the oil meniscus between them through Stokes flow and showed a decreased speed. When droplets were fully submerged into the Krytox oil, a large amount of noncoalescence droplets were observed due to the existence of the oil wrapping layer. 20,21 Surrounding the large droplets, there are many tiny non-coalescence droplets, which hinder further nucleation. Even though droplet dynamics have been extensively investigated on hydrophobic SLIPS, four fundamental challenges in condensation remain unsolved: (1) Droplet dynamics during the condensation of water vapor on hydrophilic SLIPS remains poorly understood. As SLIPS was originally developed for droplet repellency, hydrophobic but not hydrophilic oil lubricants (e.g., silicone oil, 15 Krytox oil 20) are widely used. (2) When the hydrophobic lubricant cloaks the water droplets, droplet growth and coalescence are significantly delayed.²² (3) Microdroplets with diameter $D < 20 \mu m$ cannot be rapidly removed before the contact-triggered coalescence or shedding occurs. 22,23 (4) The design guidelines to improve condensation on hydrophilic SLIPS are not clearly elucidated. In particular, the meniscus-mediated climbing effect has not been reported before.

To address those challenges, on a hydrophilic SLIPS (i.e., a hydrophilic oil-infused surface), we present a meniscus-mediated coarsening effect that enables rapid droplet coalescence and removal. We define the coarsening effect as a smaller droplet climbs spontaneously toward a larger droplet that is surrounded by oil meniscus. The unique climbing mechanism contributes to the rapid coalescence and removal, resulting in rapid droplet size evolution during condensation. We find that the coarsening-enabled droplet removal provides large water-free areas and significantly reduces the thermal resistance of condensed water. Therefore, the improved coarsening effect rapidly removes tiny droplets with diameters <20 μ m on hydrophilic SLIPS with increased lubricant thickness, which contradicts the convention that a higher thickness of liquid lubricant increases the conductive thermal resistance and hinders condensation heat transfer.

Article



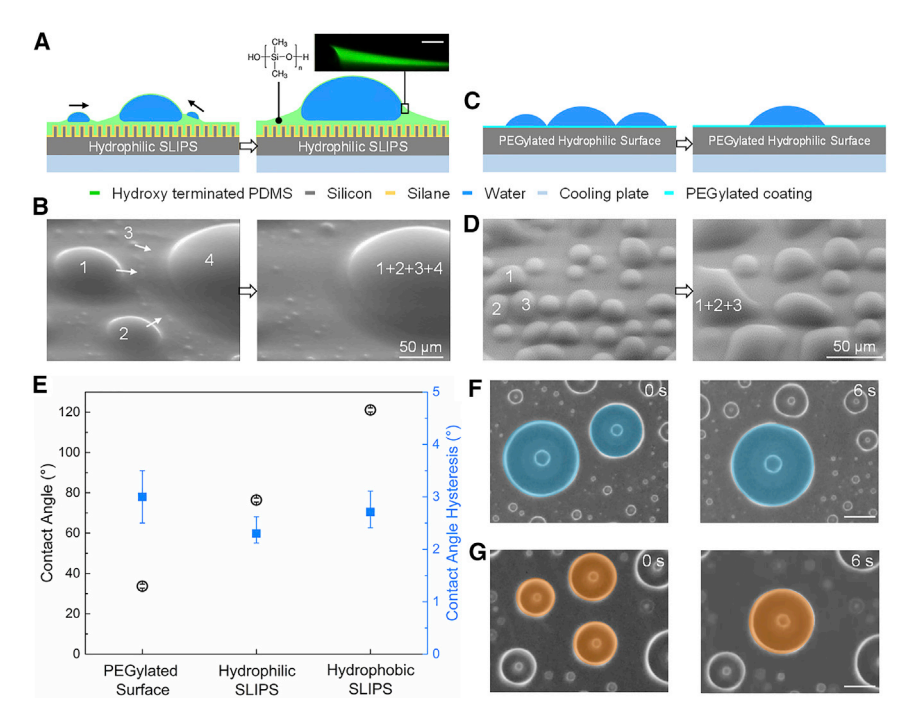


Figure 1. Coarsening droplets on hydrophilic SLIPS

(A) Schematic of coarsening droplets on hydrophilic SLIPS. Small and medium droplets move toward a larger droplet and form a coalesced droplet (moving direction shown by the arrows). The small droplet climbs on the oil meniscus. The insets are a confocal image of the oil meniscus dyed by Coumarin 6 around a water droplet, and the schematic is the chemical composition of hydroxy-terminated PDMS infused into the nanopillar. Scale bar, $200~\mu m$.

- (B) ESEM images of the coarsening droplet. The white arrows show the direction of movement of the smaller droplets 1, 2, and 3, which is toward the larger droplet 4. The right panel shows a coalesced large droplet.
- (C) Schematic of the droplet growth phenomenon on a PEGylated hydrophilic surface. Droplets need to contact others and coalesce to form a large droplet.
- (D) ESEM images of droplet coalescence on the PEGylated hydrophilic surface. Droplets 1, 2, and 3 contact each other and coalesce.
- (E) Contact angle and contact angle hysteresis of three slippery surfaces. Scale bars, 200 μm . The error bars are from the measurement uncertainties.
- $(F \ and \ G) \ Coarsening \ droplet \ is \ observed \ on \ both \ (F) \ dew \ harvesting \ and \ (G) \ fog \ harvesting \ tests \ on \ hydrophilic \ SLIPS.$

RESULTS

Coarsening droplet

Our experiments were carried out on hydrophilic SLIPS with hydroxy-terminated polydimethylsiloxane (HPDMS) as the liquid lubricant (Figure 1A; refer to Method details for details on sample preparation and setup) in a humid chamber with a cooling plate at 4°C (detailed parameters are in Experimental procedures, Dew harvesting and fog harvesting test). The hydroxy group of HPDMS provides strong electrostatic forces with water molecules. Therefore, it is more attractive to water vapor on the entire surface than other functional groups such as the trifluoromethyl group, resulting in superior vapor-to-liquid nucleation. When a water droplet is condensed or set on hydrophilic SLIPS, an oil meniscus spontaneously forms around the droplet due to the larger surface tension of water than that of HPDMS (right inset in Figure 1A). Each water droplet will be surrounded by oil meniscus due to the elastocapillary effect. 24,25 When the oil menisci are in contact, but the water droplets are not contacted, the surface tension force of the oil menisci induces spontaneous droplet



Cell Reports
Physical Science
Article

movement. Therefore, tiny droplets move toward droplets with an equivalent or larger size from all directions and coalesce with them immediately when they are in contact (<0.1 s) during dew harvesting (Figures 1A, 1B, and S1A; Video S1). Tiny water droplets climb toward their adjacent larger water droplets through the oil menisci surrounding the larger ones. This meniscus-mediated spontaneous droplet climbing on hydrophilic SLIPS leads to the rapid removal of smaller droplets and the rapid growth of larger droplets.

To elucidate the importance of the oil meniscus, we studied the droplet dynamics on a hydrophilic surface with negligible contact angle hysteresis (i.e., PEGylated hydrophilic surface²⁶). On PEGylated hydrophilic surfaces, droplet growth is dominated by either vapor adsorption or contact-triggered coalescence (Figures 1C and 1D; Video S1). Tiny droplets only grow in a fixed position before they contact adjacent droplets and coalesce to form a larger droplet, even though the water contact angle and contact angle hysteresis on the PEGylated hydrophilic surface are $38^{\circ} \pm 1^{\circ}$ and $3^{\circ} \pm 1^{\circ}$, respectively. On hydrophilic SLIPS, the water contact angle and contact angle hysteresis are $76.4^{\circ} \pm 1^{\circ}$ and $2.3 \pm 0.5^{\circ}$, respectively (Figure 1E). This shows that the oil meniscus is essential to achieving the coarsening effect.

The coarsening effect (i.e., climbing)-enabled rapid droplet coalescence is unique on hydrophilic SLIPS owing to three characteristics (Figure S1; Video S2; Supplemental experimental procedures): (1) ultra-small oil/water interfacial tension, (2) hydrophilic surface chemistry that gives a small meniscus angle, and (3) surface tension force provided by the oil meniscus. We observed the coarsening effect independently on HPDMS and ionic liquid lubricants, which have interfacial tensions with water as 7.1 and 17.8 mN/m, respectively (Figure S1). We experimentally demonstrated that microscale water droplets can float on HPDMS oil and coalesce with each other (Figure S2). This supported that water droplets could climb on the oil meniscus but not submerge in it. (If not specified, we use HPDMS oil as the hydrophilic lubricant in this work.) The coarsening effect can be identified by the climbing effect and rapid coalescence. This is distinct from the Ostwald ripening, which relies on the diffusion of a disperse phase within a bulk phase in emulsions.²⁷ As a comparison, water droplets on hydrophobic SLIPS with Krytox 101 or mineral oil show Stokes flow but not climbing. Their interfacial tensions with water are 53.8 and 50.7 mN/m, respectively. Krytox 101 forms a wrapping layer (i.e., cloaking) (Figures S3A and S3B) and mineral oil does not form a wrapping layer (Figures S3C and S3D), but the small droplets on these 2 hydrophobic SLIPS show Stokes flow and move into the oil menisci, resulting in a large drag force and noncoalescence. Such a Stokes flow prevents droplets from rapid coalescence. This indicates that the wrapping layer may be irrelevant to the climbing effect, as droplets on both Krytox 101 and mineral oil exhibit Stokes flow. The measured lubricant properties are found in Table S1. Recent work showed small satellite droplets that were condensed on large droplets on an ionic liquid-infused SLIPS, while we observed the coarsening effect. The nucleation of satellite droplets was initiated after SLIPS was fully covered by the large cloaked host droplets, 28 indicating ionic liquid formed a wrapping layer on the water droplets. This further demonstrates that the coarsening effect does not directly rely on the absence of the wrapping layer. To enhance the coarsening effect, we require a small tilted angle of oil meniscus (Figure S2) and a large driven force provided by the surface tension force of the oil lubricant. Therefore, a hydrophilic lubricant with a low oil-water interfacial tension and a high oil surface tension could enhance the coarsening effect.

To distinguish the coarsening effect with thermocapillary flow,²⁹ we performed dew harvesting with cooling (Figure 1F) and fog harvesting at room temperature

Article



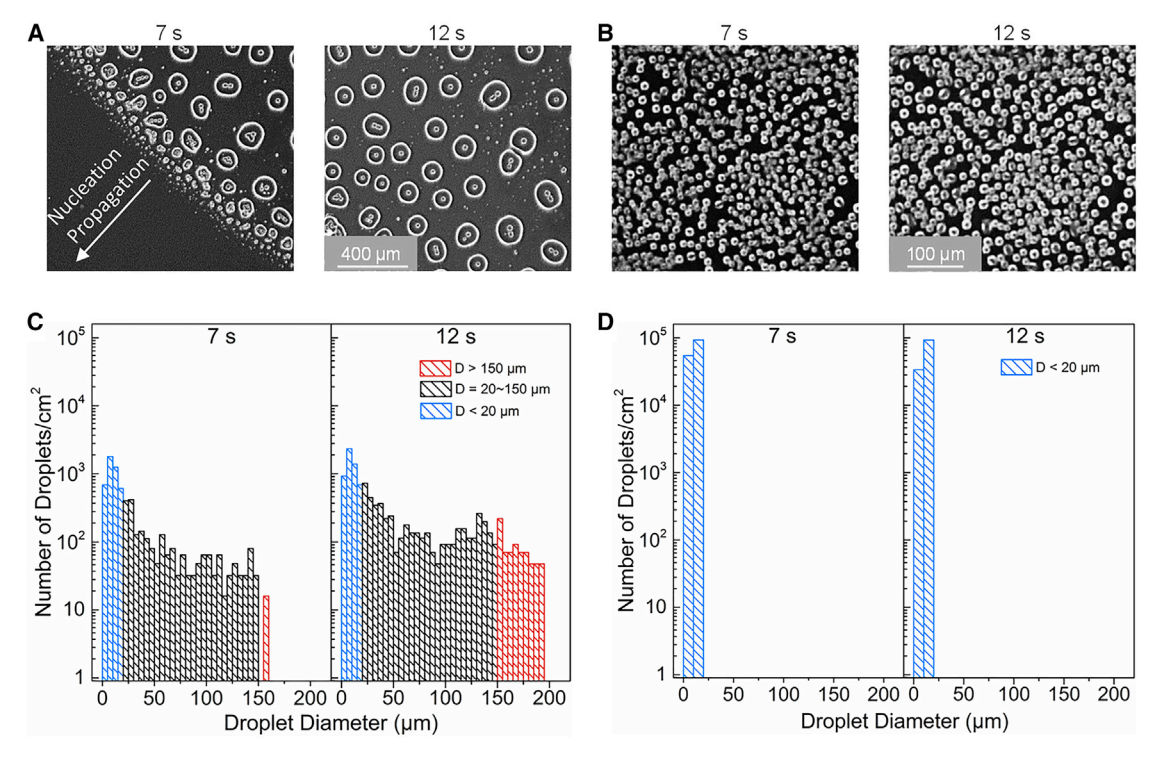


Figure 2. Droplet size distribution on different surfaces

- (A) Droplet size distribution on hydrophilic SLIPS was captured by a microscope during the dew harvesting test. It shows the coarsening effect-induced evolution of droplet size distribution with time.
- (B) Droplet size distribution on PEGylated hydrophilic surface captured by a microscope during the dew harvesting test.
- (C) The number of droplets on hydrophilic SLIPS. Tiny droplets (D \leq 20 μ m) evolve to intermediate size droplets (20 \leq D \leq 150 μ m) and giant droplets (D \geq 150 μ m).
- (D) The number of droplets on the PEGylated hydrophilic surface. It shows only tiny droplets (D \leq 20 $\mu m)$

(Figure 1G). We observed the coarsening effect during both tests. The maximum percentage of water coverage area of fog harvesting is 23%, which is lower than that of dew harvesting, at 27%, because condensation generates more tiny droplets (Figure S4; Video S3). With the oil meniscus-mediated coarsening effect, tiny droplets rapidly coalesce and form giant droplets that can be removed by gravity.

Coarsening effect enabled rapid droplet size evolution

The meniscus-mediated coarsening effect gives rise to a rapid droplet size evolution on hydrophilic SLIPS. In this work, we define droplets with diameters <20 μm as "tiny" droplets and droplets with diameters >150 μ m as "giant" droplets. The coarsening effect resulted in a large number of giant droplets immediately after nucleation on the surface (Figure 2A; Video S4). In contrast, the PEGylated hydrophilic surface is covered by a large number of tiny droplets (Figure 2B; Video S4). We found that such long-distance and fast coalescence led to an evolution of droplet size distribution with time (Figure 2C). The evolution of droplet size is not related to gravitational effects, but results mainly from the meniscus-mediated coarsening effect (Video S5). The coarsening effect increases the number of giant droplets significantly (e.g., from 16 to 510 /cm² within 5 s, as shown in Figure 2C). Meanwhile, the number of the medium-sized droplets (D = 20–150 μ m) increases from 2.3 \times 10³ to 3.5 \times 10³ /cm² (black columns, Figure 2C). The nucleation and condensation constantly occur in the water-free area and the number of tiny droplets varies slightly, from 2.5×10^5 to 2.1×10^5 /cm² (blue columns, Figure 2C). The number of tiny droplets was maintained due to the hydrophilic surface chemistry-enabled rapid nucleation. The giant



Cell Reports
Physical Science
Article

droplets also spontaneously move laterally and coalesce with each other. The coarsening effect removes tiny droplets rapidly and provides a large water-free area for further condensation/dew harvesting. On the PEGylated hydrophilic surface, the droplet size distribution evolves slightly from 7 to 12 s due to the contact-triggered droplet coalescence (Figure 2D; Video S5). Even though the hydrophilic nature of the PEGylated surface could increase the harvesting rate of water, droplets are highly pinned on the surface before coalescing and shedding. As a result, the oil meniscus-mediated coarsening effect provides giant droplets with sizes >150 μm immediately after nucleation, outperforming the PEGylated hydrophilic surface that lacks the coarsening effect.

Coarsening droplet on hydrophilic and hydrophobic SLIPS

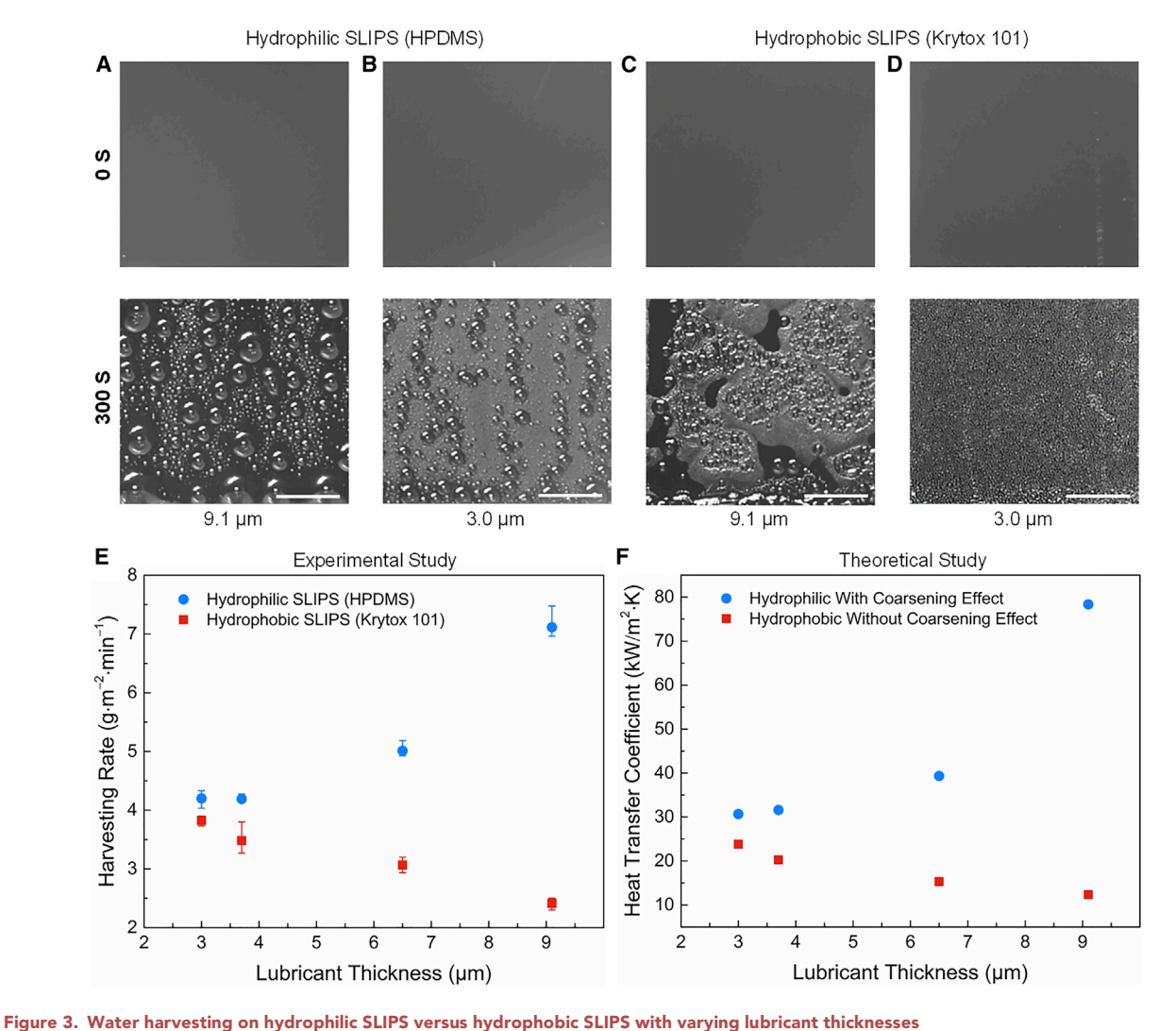
The coarsening effect significantly increases the heat transfer performance as it provides a rapid droplet size evolution and droplet removal. As HPDMS has a low thermal conductivity (\sim 0.15 W/(m • K)), a thicker HPDMS layer provides a larger thermal resistance, which results in a smaller condensation HTC or water harvesting rate. However, we showed that the water harvesting rate on hydrophilic SLIPS with a thicker lubricant is faster than the one with a thinner lubricant due to a stronger coarsening effect. To elucidate this, we studied 2 lubricants: hydrophilic lubricant² and hydrophobic lubricant, 12 with the similar thicknesses of 9.1 \pm 0.3 μm and $3.0 \pm 0.3 \,\mu\text{m}$, respectively (Figures 3A–3D). We used different spin speeds to control the thicknesses of the lubricants (Figure S5). The apparent contact angles and apparent contact angle hysteresis decreased with the increasing lubricant thickness (Figure S6). During the dew harvesting test, we observed giant droplets on the hydrophilic lubricant with a thickness of 9.1 µm (Figure 3A) forming faster than that on the one with a thickness of 3.0 μm (Figure 3B). This results from a stronger coarsening effect that enabled droplet size evolution on the hydrophilic SLIPS with a thicker lubricant. However, we observed a much smaller number of giant droplets on hydrophobic SLIPS with the lubricant thickness of 9.1 μm than that on hydrophilic SLIPS with the identical lubricant thickness (Figure 3C). On hydrophobic SLIPS with the lubricant thickness of 3.0 μm , only tiny droplets are formed on the surface without a coarsening effect (Figure 3D). The hydrophilic SLIPS with the lubricant thickness of 9.1 µm shows the strongest coarsening effect (Video S6), resulting in rapid droplet size evolution.

To quantize the impact of the coarsening effect on water harvesting, we measured the dew harvesting rate on both hydrophilic and hydrophobic SLIPS with varying lubricant thicknesses (Figure 3E). On hydrophobic SLIPS, the dew harvesting rate decreases from 3.8 to 2.4 g m $^{-2}$ min $^{-1}$ when the lubricant thickness is increased from 3.0 to 9.1 μm (i.e., increased thermal resistances) (red squares, Figure 3E). However, the dew harvesting rate increases from 4.2 to 7.1 g m $^{-2}$ min $^{-1}$ when the lubricant thickness is increased from 3.0 to 9.1 μm (i.e., increased thermal resistances) on hydrophilic SLIPS (blue dots, Figure 3E). With an identical lubricant thickness, hydrophilic SLIPS shows a higher harvesting rate than hydrophobic SLIPS due to the stronger coarsening effect-induced rapid droplet size evolution. This indicates that the dew harvesting rate is governed by the competition of the coarsening effect and thermal resistance when the lubricant thickness varies.

To elucidate the influence of the coarsening effect and thermal resistance on condensation-governed dew harvesting, we calculated the HTC of hydrophilic and hydrophobic SLIPS based on a well-developed condensation model. ^{22,30,31} Note that we used the theoretical size distribution to calculate the HTC by considering the coarsening length (see Supplemental experimental procedures). With the







(A and B) Water harvesting performance on hydrophilic SLIPS (HPDMS) during the dew harvesting test on (A) 9.1 µm lubricant thickness and (B) 3.0 µm lubricant thickness. The rapid formation of large-size droplets on the thicker lubricant results from the stronger coarsening effect.

(C and D) Water harvesting performance on hydrophobic SLIPS (Krytox 101) during the dew harvesting test on (C) 9.1 μ m lubricant thickness and (D) 3.0 μ m lubricant thickness. No large droplet was formed due to the weak coarsening effect.

- (E) Experimental study of water harvesting rate on hydrophilic and hydrophobic SLIPS performed in a humidity chamber.
- (F) Theoretical study of the heat transfer coefficient on hydrophilic and hydrophobic SLIPS during dropwise condensation.

Scale bars, 250 μ m. The thicknesses have a standard error bar of $\pm 0.3~\mu$ m. The error bars are from the measurement uncertainties.

increase in the lubricant thickness on hydrophobic SLIPS, the thermal resistance increases and leads to a reduced HTC of 23.8–12.3 kW/m² • K (red squares, Figure 3F). This trend is in line with the convention that increasing thermal resistance reduces the HTC. However, due to a stronger coarsening effect on hydrophilic SLIPS, the HTC increases from 30.6 to 78.4 kW/m² • K with the increased lubricant thickness (blue dots, Figure 3F) (see Supplemental experimental procedures). Even though a thicker lubricant layer (i.e., 9.1 μ m) has a larger thermal resistance than a thinner one (i.e., 3.0 μ m) (Figures S7 and S8), the stronger coarsening effect shows a long coalescence length. This reduces the radius of coalesced small droplets, indicating easier droplet removal. As condensed droplets are rapidly removed from the surface, the water-free area will favor further vapor nucleation on hydrophilic SLIPS due to electrostatic interactions. The theoretical study of the HTC reveals the



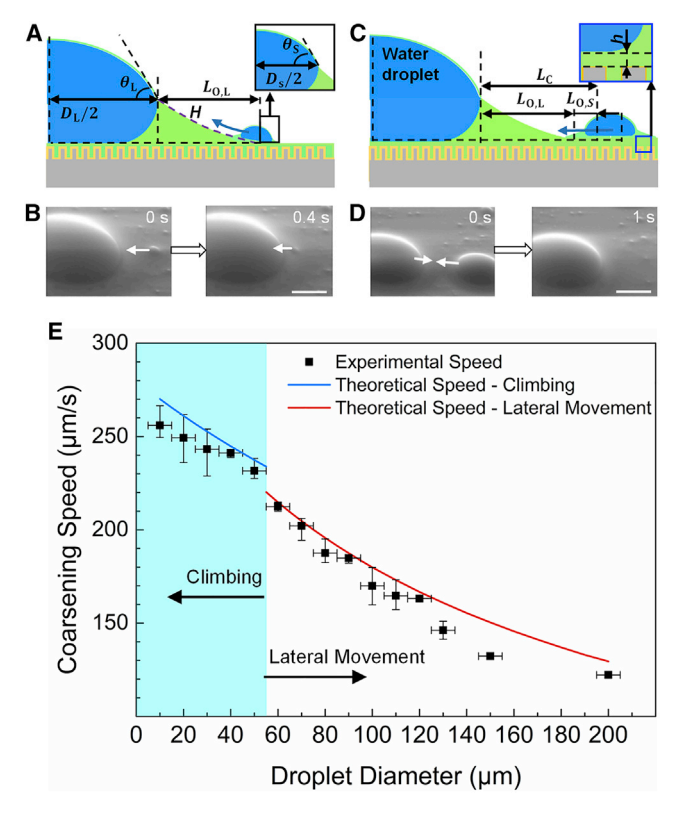


Figure 4. The mechanism of the coarsening effect on hydrophilic SLIPS

- (A) Schematic of climbing.
- (B) ESEM image of climbing. The white arrow shows the droplet movement as the water droplet climbs on the oil meniscus.
- (C) Schematic of lateral movement.
- (D) ESEM image of lateral movement. The white arrow shows the droplet movement.
- (E) Theoretical and experimental coarsening speed. Droplets in the light blue-colored area are in the climbing state. The lubricant used is hydroxy-terminated PDMS. The thickness of the lubricant is
- 9.1 μm . Scale bars, 100 μm . The error bars are from the measurement uncertainties.

importance of coarsening effect for condensation enhancement. On hydrophobic SLIPS, even though droplets could move to one another by the oil meniscus, the dense distribution of droplets significantly increases the thermal resistance. On hydrophilic SLIPS, a stronger coarsening effect is able to remove smaller sizes of droplets when the coalescence length is identical. As a result of the rapid removal of tiny droplets, the water harvesting rate and HTC are both increased with the increased lubricant thickness due to a stronger coarsening effect on hydrophilic SLIPS, despite the increased thermal resistance.

Modeling of coarsening droplet

To further understand the mechanism of the meniscus-mediated coarsening process on hydrophilic SLIPS, we divided the droplet movement into two stages: climbing (Figures 4A and 4B) and lateral movement (Figures 4C and 4D). We introduce the notation that $L_{\rm O,L}$ is the length of the oil meniscus surrounding the larger droplet, where $D_{\rm S}$ is the diameter of the smaller droplet. When $L_{\rm O,L} > D_{\rm S}$, and the smaller droplet is in contact with the meniscus of the larger droplet, the smaller droplet will move laterally toward the larger droplet and climb on the oil meniscus (Figures 4A and 4B; Video S7, left). When $L_{\rm O,L} < D_{\rm S}$, the 2 droplets move laterally toward each other and coalesce (Figures 4C and 4D; Video S7, right). Once the menisci of those

Article



droplets are connected, they will spontaneously move toward each other. Compared with the well-known Cheerios effect³² (i.e., solid particles move laterally toward one another³³), our meniscus-mediated droplet movement exhibits three characteristics: (1) the water droplet shows both climbing and lateral movement, depending on the droplet diameters on hydrophilic SLIPS; (2) the water droplets could coalesce immediately when they contact one another; and (3) the meniscus-mediated coalescence leads to the rapid removal of smaller droplets and enhances the growth of larger droplets. Moreover, due to the coarsening effect, smaller droplets can move toward larger droplets and coalesce with them from all directions, regardless of the surface orientation (Videos S5 and S7).

To provide quantitative design rules for the coarsening effect, we studied the physical mechanisms of the climbing and lateral movement processes. We simplified the coarsening effect and only focused on two droplets, as shown in Figures 4A and 4C, where D_L and D_S are the diameters of the larger and smaller droplets, respectively; θ_L and θ_S are apparent contact angles of the larger and smaller droplets, respectively; $L_{O,L}$ and $L_{O,S}$ are the meniscus lengths of the larger and smaller droplets, respectively; H(x) is the meniscus shape function based on the length of oil meniscus L_O ; h is the lubricant thickness; and $L_C = L_{O,L} + L_{O,S}$ is the "coarsening length" between two droplets (Figure 4C). In the modeling, we simplified the droplets as a sphere shape for calculation. The driving force for lateral movement in the x-direction (see Supplemental experimental procedures) studied in a previous paper³⁴ is

$$F_{\rm x} = F_{\rm s,x} = 2\pi\gamma_{\rm ov} \frac{O_{\rm L}O_{\rm S}}{\rm x}$$
 (Equation 1)

where F_x is the force component in the x-direction; x is the distance between 2 droplets, with $0 \le x \le L_C$; $F_{s,x}$ is the surface tension force component in the x-direction of the oil meniscus surrounding the water droplet; γ_{ov} is the oil-vapor interfacial tension (i.e., 21.2 mN/m for HPDMS); and Q_L and Q_S are the "capillary charges" of larger and smaller droplets, respectively. The capillary charge relates to the contact angle of the water droplet on oil lubricants (Equation S18 in Supplemental experimental procedures). Here, we assume that the contact angles of those droplets are the same as the static contact angle (i.e., 64°) on the hydrophilic SLIPS.

When the smaller water droplet climbs the oil meniscus of the larger water droplet, there is one additional force applied on the smaller droplet due to the tilting of the oil meniscus while the lateral force acts on the smaller droplet. As shown in Table S2, the Bond number (Bo) = 8.4 \times 10 $^{-3}$ << 1 for water droplets with diameters no more than 150 μm . The interfacial tension force dominates, and gravitational force can be neglected. Thus, the climbing droplet can be simplified as it moves on the oil meniscus that surrounds a larger droplet. Then, the total driving force for the climbing droplet is

$$F_x = F_{s,x} + F_{p,x}$$
 (Equation 2)

where $F_{\rm s,x}$ is the lateral movement force in Equation 1, including the contribution from forces due to the interface (Figures S9 and S10), and $F_{\rm p,x}$ is the simplified force of hydrostatic pressure of the oil meniscus acting on the smaller water droplet in the x-direction (Equations S18, S19, S20, S21, S22, S23, S24, S25, S26, S27, S28, and S29 in Supplemental experimental procedures). Figure S9 shows the surface tension contribution and simplified force of the hydrostatic pressure components in the x-direction due to the tilting of the smaller water droplets on the oil meniscus. The driving force for lateral movement in Equation 1 is given by Equation 2, with $F_{\rm p,x}$ = 0. While the smaller water droplet moves laterally on the oil-infused surface, there



Cell Reports
Physical Science
Article

is a layer of oil lubricant underneath the water droplet, which generates a drag force dependent on the droplet size and speed.^{36,37} As the height of the oil meniscus is smaller than the droplet height, we assume that the oil meniscus moves underneath the droplet, which is not the Stokes flow in this case, and is different from the droplet movement on Krytox oils.²⁰ For a coarsening droplet, the climbing time is <1 s (Figure 4B). Moreover, the thickness under the moving droplet predicted by Landau-Levich entrainment is similar to the meniscus height. In this case, the underneath thickness could be simplified with the drag force for average speed (Supplemental experimental procedures). Thus, the drag force is estimated as:

$$F_{\rm d} \approx \pi \gamma_{\rm lo} D_{\rm S} Ca^{2/3}$$
 (Equation 3)

where $Ca = \eta U/\gamma_{1o}$ is the capillary number, γ_{1o} is the interfacial tension of water and oil, η is the viscosity of the lubricant, and U is the speed of the water droplet. During the coarsening process, climbing occurs within 1 s, and the distance between the 2 water droplets is <200 μ m. Thus, the Reynolds number of the smaller droplet is $R_e = (\rho U D_s/\mu)$, where $\rho = 998$ kg/m³ is the density and $\mu = 1.5$ N · s/m² is the dynamic viscosity of water at 4°C, U = 200 μ m/s is the speed of the water droplet, and $D_s = 100$ μ m is the diameter of the droplet. Thus, $R_e = 10^{-4} << 1$ shows that the convective inertial effects are much smaller than the viscous effects, ³⁸ and the acceleration of the droplet could be ignored. To attain the coarsening speed for both climbing and lateral movement water droplets, the driving force is equal to the drag force as $F_d = F_x$. Therefore, the theoretical coarsening speed U of the smaller water droplet as a function of distance x is (see Supplemental experimental procedures)

$$U = \frac{\gamma_{lo}}{\eta} \left(\frac{\gamma_{ov}}{\gamma_{lo}} \frac{Q_2 Q_1}{Rx} + \frac{\gamma_{ov}}{\gamma_{lo} R} Q_2 \frac{1}{L_{O,L}} H(x) + \frac{\gamma_{ov}}{2\gamma_{lo} R} \frac{1}{L_{O,L}} \left(\frac{D_S}{2} \frac{1}{L_{O,L}} H(x) \right)^2 \right)^{\frac{3}{2}}$$
 (Equation 4)

where H(x) is the height of the oil meniscus at distance $0 \le x \le L_R$ between the smaller and larger droplets (Figure S10). As we measured the experimental coarsening speed based on the distance and time of the movements on SLIPS with a lubricant thickness of 9.1 μ m, we simplified the average theoretical coarsening speed Ushown as Equation S29 in the Supplemental experimental procedures. In this case, to obtain a reliable speed, we fixed the diameter of the larger water droplet D_L = 200 µm and then measured the speed of smaller water droplets with diameters from 10 to 200 μm. The experimental coarsening speed and theoretical coarsening speed \overline{U} show good agreement both in climbing and lateral movement processes (Figure 4E). Note that the critical droplet diameter between the lateral movement and climbing is hard to determine experimentally, leading to a sharp transition. The light blue area in Figure 4E is the coarsening speed for climbing droplets, with $D_{\rm S} \leq 55~\mu{\rm m} < L_{\rm O,L}$, while a droplet could only be in the lateral movement when $L_{O,L} < D_S$. The experimental coarsening speed of the self-climbing droplet could reach as high as 250 \pm 10 μ m/s at D_S = 10 μ m showing a higher speed than lateral movement.

Coarsening speed and coarsening length

We define the speed of a coarsening droplet as average coarsening speed and instantaneous coarsening speed. The instantaneous speed is the speed of the droplet at a certain position, which depends on the distance x between larger and smaller droplets shown in Equation 4. Meanwhile, the average coarsening speed is the integral of instantaneous speed along the moving direction, which includes both lateral and climbing movement. We measured the average coarsening speed based on the coarsening length (L_C) between two droplets (i.e., the distance between red-dashed circles of 1 and 2) (Figure 5A). When the oil menisci start to

Article



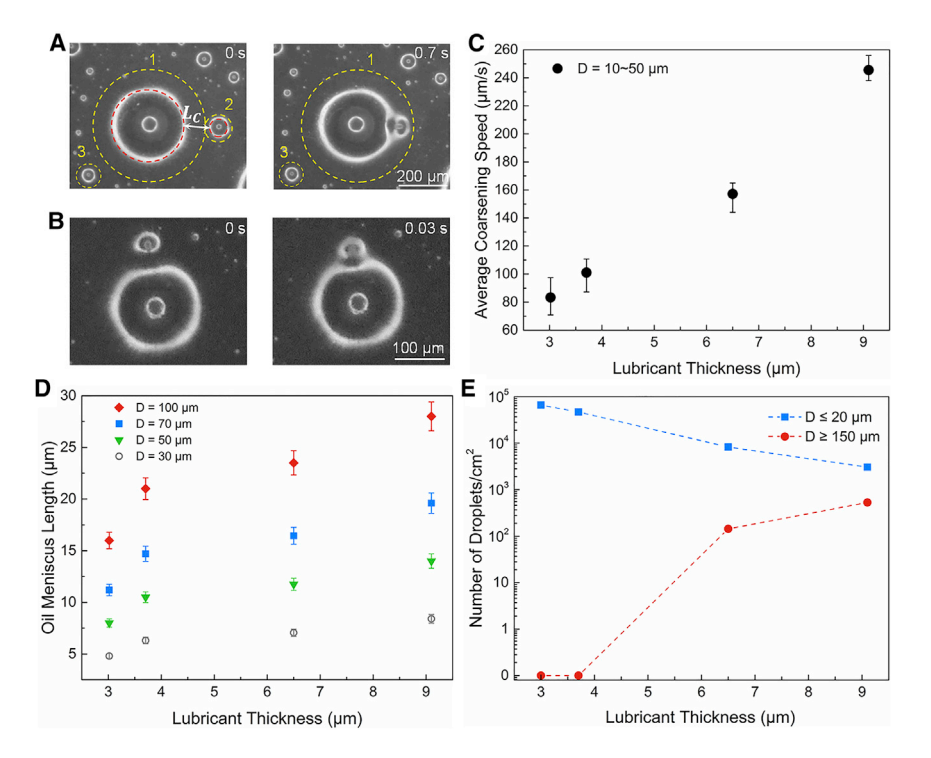


Figure 5. The dynamics of coarsening droplets on hydrophilic SLIPS with varying lubricant thicknesses

(A) Average coarsening speed: coarsening length over the total time of lateral movement and climbing. The coarsening length ($L_{\rm C}$) shown as the white arrow is the distance between two droplets. The red dashed circle denotes a droplet, and the yellow dashed circle denotes an oil meniscus surrounding a droplet.

(B) Instantaneous coarsening speed: the coarsening speed of a smaller droplet at a certain position. Here, we chose the position that is closest to the larger droplet, which shows the highest instantaneous coarsening speed due to climbing.

- (C) Average coarsening speed depends on lubricant thickness.
- (D) Oil meniscus length depends on lubricant thickness. Selected droplet diameters are 30, 50, 70, and 100 μm .
- (E) Coarsening effect increased the number of giant droplets (D $\geq 150~\mu m)$ and reduced the number of tiny droplets (D $\leq 20~\mu m)$ on hydrophilic SLIPS with increasing lubricant thickness. The data were collected 20 s after first nucleation on the surfaces. The error bars are from the measurement uncertainties.

contact (i.e., the yellow-dashed circles of 1 and 2 are tangent in Figure 5A), droplet 2 starts moving toward droplet 1. Then, we calculated the average coarsening speed as $\overline{U} = L_{C/t}$, where t is the time for droplet 2 to droplet 1. Meanwhile, the instantaneous coarsening speed increases when the smaller droplet is close to the larger droplet (climbing), showing a higher speed (\sim 1,200 µm/s; Figure 5B) than the average coarsening speed (\sim 230 µm/s, D = 50 µm; Figure 4E). The smaller droplet is accelerated when it moves close to the larger droplet in the climbing process on hydrophilic SLIPS (Figure 5B). However, droplets on hydrophobic SLIPS show a sharp deceleration of speed from 800 to 0 µm/s when they are close to the larger droplets. While the instantaneous coarsening speed varies at different positions, the average coarsening speed is more appropriate to characterize the speed during the entire coarsening process.

As the lubricant thickness significantly influenced the coarsening effect (Figure 3), we quantified the average coarsening speed on hydrophilic SLIPS with the lubricant



Cell Reports
Physical Science
Article

thicknesses of 3.0, 3.7, 6.5, and 9.1 \pm 0.3 μ m, where the average coarsening speed of the smaller coarsening droplets (D = 10–50 μ m) are 80, 110, 200, and 250 μ m/s, respectively (Figure 5C). When the lubricant thickness is increased from 3.0 to 9.1 μ m, the coarsening speed is increased by 210%, showing a stronger coarsening effect.

We also found that the oil meniscus length $L_{\rm O}$ surrounding a water droplet is equally important as the coarsening speed. As the coarsening effect requires the contact of oil menisci, a larger water droplet with a longer coarsening length could potentially harvest a larger area of smaller water droplets. Therefore, there are no droplets within the oil meniscus length, which provides a larger water-free area for sustainable condensation. Here, 4 different diameters, $D = 30, 50, 70, \text{ and } 100 \,\mu\text{m}$, are chosen to show the oil meniscus length of a single droplet (Figures 5D and S11). A larger oil meniscus length on a thicker SLIPS enables a tiny droplet to move over larger distances for generating giant droplets. As a consequence of increased lubricant thickness, which shows a higher coarsening speed and longer coarsening length, the number of the droplets <20 μm decreases significantly from 6.5 \times 10⁴ to 3.1 \times 10³/cm², and the number of giant droplets (Figure 5E) increases from 0 to 530/ cm² (Figure S12; Video S8). The number of giant droplets formed during the given time indicates that the coarsening effect effectively removes the tiny water droplets on the hydrophilic SLIPS. A thicker lubricant layer $h = 9.1 \mu m$ shows a stronger coarsening effect, which is visualized by a smaller number of tiny droplets and a high density of the giant droplets. This phenomenon is determined by the drag force, which strongly depends on the lubricant thickness. Once the smaller water droplet moves on SLIPS, a shear force will be applied in the lubricant layer underneath the droplet. When two droplets move on the lubricant at the same velocity, the drag force caused by the thinner lubricant will be larger due to a larger velocity gradient in the lubricant layer $\tau = \mu(du/dy)$, where μ is the viscosity of the oil lubricant, (du/dy) is the velocity gradient within the oil lubricant, and τ is the shear stress. As a consequence, a thinner lubricant layer will decrease the coarsening effect due to the higher drag force and smaller oil meniscus length. A strong coarsening effect will show a high coarsening speed with a long coarsening length.

Coarsening effect enhanced dew harvesting

The coarsening effect occurs on SLIPS with different coarsening speeds, but not on the PEGylated hydrophilic surface (Figures 6A and S13; Video S9). Hydrophilic SLIPS shows a higher average coarsening speed ($U \approx 250 \, \mu \text{m/s}$) enhanced by climbing, while hydrophobic SLIPS shows a lower speed ($U \approx 130 \, \mu \text{m/s}$). There is no droplet movement on the PEGylated hydrophilic surface. The hydrophilic SLIPS also showed the largest number of giant droplets due to the strongest coarsening effect (Figure 6B; Video S9). Based on the driving force in Equation 2, a larger contact angle provides a smaller force for lateral movement. In addition, when water droplets are on the hydrophobic SLIPS, the length of the oil meniscus may be smaller or identical to the diameter of the water droplet, which leads to the smaller droplet not climbing. With a small oil meniscus, the coarsening effect is weak, so large droplets can still contact one another directly. On hydrophilic SLIPS, the coarsening effect generates a large number of giant droplets. Therefore, the percentage of water coverage area is maintained at ~30% before droplet shedding (Figure 6C). On hydrophobic SLIPS, the percentage of coverage area is 14% at the beginning, which is smaller than that on hydrophilic SLIPS. This is due to poor nucleation on the hydrophobic lubricant. Due to the weak coarsening effect and the existence of non-coalescence droplets, the percentage of the coverage area increased before the droplet shedding, demonstrating an average percentage of coverage area of 51%

Article



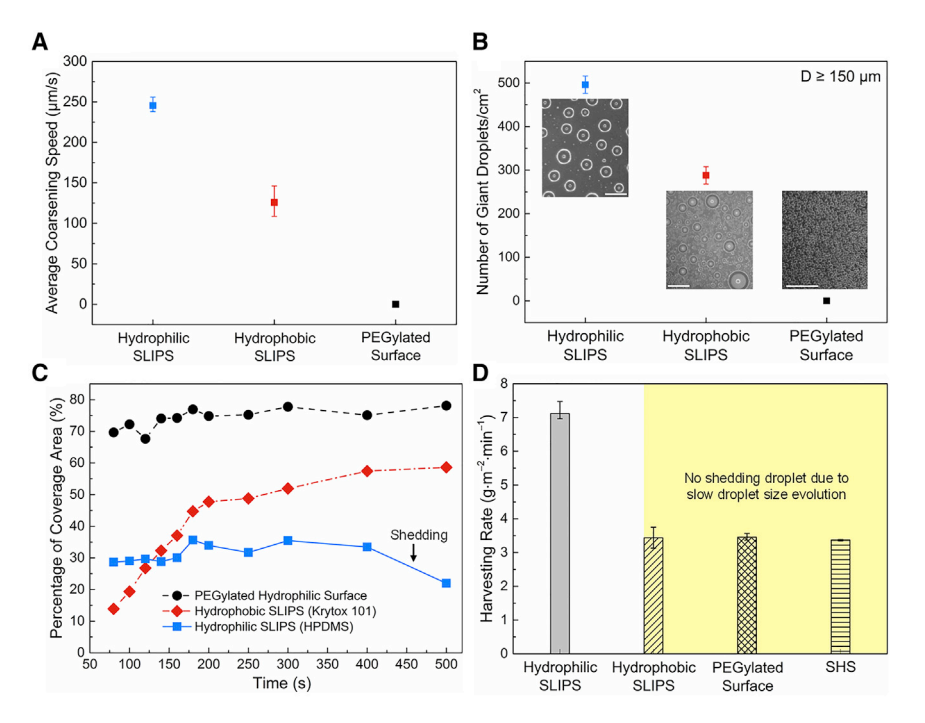


Figure 6. Coarsening effect enabled rapid water harvesting

- (A) Coarsening speed varies with the choice of the surfaces. No coarsening effect on PEGylated hydrophilic surface with a negligible contact angle hysteresis. The coarsening speed is measured for droplets with a diameter of 10– $50~\mu m$.
- (B) The number of droplets >150 μ m varies with the surfaces. The inset images show a part of the surfaces with the large droplets. The scale bars are 500 μ m for inserted images. The data were collected 20 s after the first nucleation on the surfaces.
- (C) The percentage of water coverage area varies for different surfaces during the dew harvesting test. The starting time is the first nucleation that occurs on the surfaces. The arrow points out that the droplet shedding decreases the coverage area.
- (D) Dew harvesting rates on hydrophilic SLIPS, hydrophobic SLIPS, PEGylated surface, and SHS. All of the tests are condensation-driven dew harvesting. No droplet shedding in the yellow region due to slow droplet size evolution during the 5 min dew harvesting tests. The error bars are from the measurement uncertainties.

(Figure 6C). However, on the PEGylated hydrophilic surface, droplet growth relied only on vapor absorption and contact-triggered coalescence, so small droplets are densely distributed. Therefore, the percentage of water coverage area is 74%, which is 150% larger than that on hydrophilic SLIPS (Figure 6C). Hence, there was a small water-free area for further vapor nucleation. We also observed that droplet shedding only occurred on hydrophilic SLIPS during the dew harvesting test for 500 s. This resulted from the rapid coarsening effect that enabled droplet size evolution. Thus, droplets could easily reach the shedding diameter and shed off on hydrophilic SLIPS, which further reduced the water coverage (Figures 6C and S13; Video S9).

Due to the strong coarsening effect for removing tiny droplets and gravity-assisted shedding of giant droplets, ¹³ the dew harvesting rate on hydrophilic SLIPS is 200% and 219% higher than those on hydrophobic SLIPS and PEGylated hydrophilic surface, as well as 220% higher than that on the SHS (Figure 6D). There was no droplet shedding on the hydrophobic SLIPS and the PEGylated hydrophilic surface, so they showed a nearly identical harvesting rate. With a high coarsening speed and large coarsening length, the nucleated tiny droplets could spontaneously move toward



Cell Reports
Physical Science
Article

and coalesce with larger ones, resulting in a large water-free area for further vapor condensation. Thus, the coarsening effect-enabled rapid removal of tiny water droplets on hydrophilic SLIPS results in the highest harvesting rate.

DISCUSSION

We reported a meniscus-mediated spontaneous droplet climbing and rapid coalescence on hydrophilic SLIPS, which we characterize as a coarsening effect. The self-generated oil menisci surrounding water droplets can provide a bridge for droplets with sizes <20 μm to climb toward and coalesce with the larger droplets. The coarsening effect enabled rapid droplet climbing, and coalescence without any external energy or temperature gradient is unique on hydrophilic SLIPS, which results in rapid droplet size evolution and small water coverage area during the condensation process. Droplets with sizes >150 µm can rapidly form and shed from hydrophilic SLIPS, providing large water-free areas for further vapor condensation. The fundamental driving force for the coarsening effect results from the surface tension force and oil meniscus-mediated capillary force acting on water droplets. In particular, an increased oil thickness improves the coarsening speed and coarsening length (i.e., smaller droplets can climb the oil menisci and coalesce with the larger droplets faster). To enhance the coarsening effect, a hydrophilic lubricant with low interfacial tension and a high oil surface tension is preferred. There also exists a trade-off between the coarsening effect and thermal resistance. Although an increased thickness of hydrophilic lubricant provides a larger thermal resistance, the stronger coarsening effect-assisted droplet removal significantly reduces the thermal resistance of condensed water, giving rise to rapid nucleation and droplet size evolution. Therefore, a slightly thicker lubricant leads to a higher heat transfer performance, although its conductive thermal resistance is slightly higher. As a result, the rapid removal of smaller droplets and fast shedding of larger droplets on hydrophilic SLIPS maintain a percentage of water coverage <~30% for dropwise condensation. This, in turn, provides a higher water harvesting rate on hydrophilic SLIPS than those on hydrophobic SLIPS, the PEGylated hydrophilic surface, and the SHS.

This work focused on the fundamental elucidation of the coarsening effect (i.e., meniscus-mediated climbing), which will provide a theoretical guideline for surface design. The current HPDMS-enabled hydrophilic SLIPS suffers from lubricant depletion after 4 h during dew harvesting. Creating a durable coarsening surface is a potential research direction in this area. We envision that our fundamental understanding will provide design guidelines to make artificial surfaces for the coarsening effect, which will pave a way for water harvesting, condensation, and refrigeration applications.

EXPERIMENTAL PROCEDURES

Resource availability

Lead contact

Further information and requests for resources should be directed to and will be fulfilled by the lead contact, Xianming Dai (dai@utdallas.edu).

Materials availability

All unique surfaces generated in this study are available from the lead contact without restriction.

Data and code availability

All data are available from the lead contact upon reasonable request.

Article



Preparation of SHSs

The nanostructures (Figure S14) on SHSs were fabricated on a 10 cm < 100 > ptype silicon (Si) wafer (Nova Electronic Materials) with a thickness of 450 μm . Cleaned Si wafers were immediately immersed into a solution of 4.8 M hydrofluoric acid (HF) and 0.01 M silver nitrate (AgNO3) for 1 min to deposit catalysts. The silver ions (Ag $^+$) were reduced to Ag nanoparticles, which deposited on the Si surfaces and acted as catalysts to enhance local etching. The wafer with catalyst was placed in the etching solution containing 4.8 M HF and 0.3 M hydrogen peroxide (H₂O₂) for 4 min, which gave a 1- μ m depth of the nanostructures. After the etching, the wafers were placed into a 30% diluted nitric acid (HNO3) solution to dissolve the Ag nanoparticle. Then, the wafer was washed with deionized water (DI water) and dried with nitrogen (N₂) gas. Finally, the nanostructured black Si was silanized by chlorotrimethylsilane (Sigma-Aldrich) in the vapor phase to make superhydrophobic surfaces.

Preparation of SLIPS

Oil lubricant was spin coated on the SHSs to form liquid-infused surfaces by a spin coater (Laurell WS-650-23B). The spin speed determined the thickness of the oil lubricant (Figure S5). Hydroxy-terminated poly(dimethylsiloxane) (average Mn $\sim\!550$, viscosity $\sim\!25$ cSt) was purchased from Sigma-Aldrich. The ionic liquid (1-butyl-1-methylpyrrolidinium bis (trifluoromethylsulfonyl) imide [BMP-BTI]) was purchased from TCI Chemicals. Perfluorinated fluid (Krytox GPL 101) was obtained from DuPont. Carnation white mineral oil was obtained from Sonneborn.

Preparation of PEGylated hydrophilic surface

We followed the recipe reported in a previous paper. ²⁶ Cleaned Si wafers were exposed to oxygen (O_2) plasma for 15 min and subsequently immersed in a solution consisting of 1 μ L 2-[methoxy(polyethyleneoxy)6-9propyl]trimethoxysilane (Gelest) and 8 μ L hydrochloric acid (Fisher Chemical) in 10 mL anhydrous toluene (VWR) for 18 h at room temperature. Lastly, the PEGylated surfaces were rinsed with anhydrous toluene, ethanol, and DI water and stored in DI water for further use.

Dew harvesting and fog harvesting tests

A self-built chamber was used for the condensation test at atmospheric pressure (1 atm). For the dew harvesting test, a cooling plate was added underneath SLIPS to generate and harvest tiny droplets, which was controlled by a chiller (NESLAB RTE111). The humidity was 95% \pm 3%, generated by a humidifier (Crane Drop Ultrasonic Cool Mist Humidifier). The room temperature (water vapor temperature) was 22°C and the dew point was 20°C. The sample temperature was 4°C, the same as the cooling plate temperature. The videos and images were captured using a Nikon camera (D5600) assembled with a microscope (Amscope 7X-45X Binocular Stereo Zoom microscope). We measured the weight of the substrate before and after the dew harvesting test to calculate the dew harvesting rate. The fog harvesting test was performed at room temperature (20°C–22°C) with a humidifier.

Fluorescence confocal microscopy

To test the lubricant thickness and meniscus shape on the lubricated black Si surface, the FV-MPE Multiphoton Microscope (Olympus MPE-RS TWIN) was used. Lubricants were dyed by Coumarin 6 (TCI Chemical) at a weight concentration of 1% with further filtration. The power was fixed as 9% with voltage 560 V. The infrared (IR) laser wavelength was 900 nm and the fluorescence filter was U-FGW (green, 530–550/570/575 LP). Water droplets were not dyed.



Cell Reports
Physical Science
Article

Contact angle and surface tension measurements

The contact angle measurements and the surface tension measurements were carried out using a standard goniometer (model 290, ramé-hart instrument) at room temperature under ambient conditions (20°C–22°C, ~50 % relative humidity). All of the contact angle values were averaged from at least 5 independent measurements by applying ~5 μL droplets on the test platform. With the change in the lubricant thickness, the contact angles change at the same time. In Figure S6A, the apparent water contact angles on hydrophilic SLIPS are 64.2°, 65.7°, 72.4°, and 76.4° for lubricant thickness of 9.1 \pm 0.3 μm , 6.5 \pm 0.3 μm , 3.7 \pm 0.3 μm , and 3.0 \pm 0.3 μm , respectively. In Figure S6B, the apparent water contact angles on hydrophobic SLIPS are 113.4°, 115.5°, 117.5°, and 121.3°, for lubricant thickness of 9.1 \pm 0.3 μm , 6.5 \pm 0.3 μm , and 3.0 \pm 0.3 μm , respectively. For surface tension measurements, we used the pendant droplet method. The measurement stand error is \pm 1 mN/m.

Environmental SEM

The oil-infused nanotextured surface was visualized using an environmental scanning electron microscope (ESEM, Zeiss EVO LS 15 SEM) on a Peltier cooling angled stage (tilted at 60°). The applied voltage was 20 kV and the current was 2.1 nA for the operation. The pressure was set to 3.8 torr, and the temperature was fixed at $-4.5^{\circ}\text{C} \pm 0.5^{\circ}\text{C}$.

SUPPLEMENTAL INFORMATION

Supplemental Information can be found online at https://doi.org/10.1016/j.xcrp. 2021.100387.

ACKNOWLEDGMENTS

Z.G., D.M., and X.D. acknowledge the National Science Foundation (award no. 1929677), and the Young Investigator Program at the Army Research Office (award no. W911NF1910416). L.Z. and X.D. acknowledge the startup funding support by the University of Texas at Dallas (UT Dallas). This project was partially funded by the Office of Research at UT Dallas through the Core Facility Voucher Program. X.D. acknowledges the discussion with Jonathan Boreyko at the 71st Annual Meeting of the American Physical Society's Division of Fluid Dynamics (DFD). Z.G. and X.D. acknowledge the discussion with Ping He. Jyotirmoy Sarma's proofreading is greatly appreciated.

AUTHOR CONTRIBUTIONS

X.D. conceived the research. X.D. and H.A.S. supervised the research. Z.G. and X.D. designed the experiments. Z.G. and L.Z. carried out the experiments. Z.G., D.M., and X.D. analyzed the data. Z.G., H.A.S., and X.D. developed the droplet movement model. Z.G., D.M., and X.D. developed the heat transfer model. Z.G., L.Z., D.M., H.A.S., and X.D. wrote and revised the manuscript.

DECLARATION OF INTERESTS

The authors declare no competing interests.

Received: October 6, 2020 Revised: January 12, 2021 Accepted: March 4, 2021 Published: March 25, 2021

Article



REFERENCES

- Park, K.-C., Kim, P., Grinthal, A., He, N., Fox, D., Weaver, J.C., and Aizenberg, J. (2016). Condensation on slippery asymmetric bumps. Nature 531, 78–82.
- Dai, X., Sun, N., Nielsen, S.O., Stogin, B.B., Wang, J., Yang, S., and Wong, T.-S. (2018). Hydrophilic directional slippery rough surfaces for water harvesting. Sci. Adv. 4, eaaq0919.
- 3. Hou, Y., Yu, M., Chen, X., Wang, Z., and Yao, S. (2015). Recurrent filmwise and dropwise condensation on a beetle mimetic surface. ACS Nano 9, 71–81.
- Bai, H., Wang, L., Ju, J., Sun, R., Zheng, Y., and Jiang, L. (2014). Efficient water collection on integrative bioinspired surfaces with starshaped wettability patterns. Adv. Mater. 26, 5025–5030.
- Kim, H., Yang, S., Rao, S.R., Narayanan, S., Kapustin, E.A., Furukawa, H., Umans, A.S., Yaghi, O.M., and Wang, E.N. (2017). Water harvesting from air with metal-organic frameworks powered by natural sunlight. Science 356, 430–434.
- Bergman, T.L., Lavine, A.S., Incropera, F.P., and DeWitt, D.P. (2017). Fundamentals of Heat and Mass Transfer (Wiley).
- Rose, J. (2002). Dropwise condensation theory and experiment: a review. Proc. Inst. Mech. Eng. Part A 216, 115–128.
- Boreyko, J.B., and Chen, C.-H. (2009). Selfpropelled dropwise condensate on superhydrophobic surfaces. Phys. Rev. Lett. 103. 184501.
- Wen, R., Lan, Z., Peng, B., Xu, W., Yang, R., and Ma, X. (2017). Wetting transition of condensed droplets on nanostructured superhydrophobic surfaces: coordination of surface properties and condensing conditions. ACS Appl. Mater. Interfaces 9, 13770–13777.
- Angelescu, D., Moscato, T., Pauchet, F., and Van Kujik, R. (2010). A micro-structured surface having tailored wetting properties. US patent WO201028752, filed August 24, 2009, and published March 18, 2010.
- Lafuma, A., and Quéré, D. (2011). Slippery presuffused surfaces. Europhys. Lett. 96, 56001.
- Wong, T.-S., Kang, S.H., Tang, S.K., Smythe, E.J., Hatton, B.D., Grinthal, A., and Aizenberg, J. (2011). Bioinspired self-repairing slippery surfaces with pressure-stable omniphobicity. Nature 477, 443–447.
- Anand, S., Paxson, A.T., Dhiman, R., Smith, J.D., and Varanasi, K.K. (2012). Enhanced condensation on lubricant-impregnated

- nanotextured surfaces. ACS Nano 6, 10122–10129.
- Xiao, R., Miljkovic, N., Enright, R., and Wang, E.N. (2013). Immersion condensation on oilinfused heterogeneous surfaces for enhanced heat transfer. Sci. Rep. 3, 1988.
- Anand, S., Rykaczewski, K., Subramanyam, S.B., Beysens, D., and Varanasi, K.K. (2015). How droplets nucleate and grow on liquids and liquid impregnated surfaces. Soft Matter 11, 69–80.
- Hui Guan, J., Ruiz-Gutiérrez, É., Xu, B.B., Wood, D., McHale, G., Ledesma-Aguilar, R., and George Wells, G. (2017). Drop transport and positioning on lubricant-impregnated surfaces. Soft Matter 13, 3404–3410.
- Orme, B.V., McHale, G., Ledesma-Aguilar, R., and Wells, G.G. (2019). Droplet Retention and Shedding on Slippery Substrates. Langmuir 35, 9146–9151.
- Jiang, J., Gao, J., Zhang, H., He, W., Zhang, J., Daniel, D., and Yao, X. (2019). Directional pumping of water and oil microdroplets on slippery surface. Proc. Natl. Acad. Sci. USA 116, 2482–2487
- Zhang, X., Sun, L., Wang, Y., Bian, F., Wang, Y., and Zhao, Y. (2019). Multibioinspired slippery surfaces with wettable bump arrays for droplets pumping. Proc. Natl. Acad. Sci. USA 116, 20863–20868.
- Sun, J., and Weisensee, P.B. (2019). Microdroplet self-propulsion during dropwise condensation on lubricant-infused surfaces. Soft Matter 15, 4808–4817.
- Boreyko, J.B., Polizos, G., Datskos, P.G., Sarles, S.A., and Collier, C.P. (2014). Air-stable droplet interface bilayers on oil-infused surfaces. Proc. Natl. Acad. Sci. USA 111, 7588–7593.
- Weisensee, P.B., Wang, Y., Hongliang, Q., Schultz, D., King, W.P., and Miljkovic, N. (2017). Condensate droplet size distribution on lubricant-infused surfaces. Int. J. Heat Mass Transf. 109, 187–199.
- Enright, R., Miljkovic, N., Sprittles, J., Nolan, K., Mitchell, R., and Wang, E.N. (2014). How coalescing droplets jump. ACS Nano 8, 10352– 10362
- 24. Pericet-Cámara, R., Best, A., Butt, H.J., and Bonaccurso, E. (2008). Effect of capillary pressure and surface tension on the deformation of elastic surfaces by sessile liquid microdrops: an experimental investigation. Langmuir 24, 10565–10568.
- Bico, J., Reyssat, É., and Roman, B. (2018).
 Elastocapillarity: when surface tension deforms

- elastic solids. Annu. Rev. Fluid Mech. 50, 629–659.
- Cha, H., Vahabi, H., Wu, A., Chavan, S., Kim, M.K., Sett, S., Bosch, S.A., Wang, W., Kota, A.K., and Miljkovic, N. (2020). Dropwise condensation on solid hydrophilic surfaces. Sci. Adv. 6, eaax0746.
- Taylor, P. (1998). Ostwald ripening in emulsions. Adv. Colloid Interface Sci. 75, 107–163.
- Ge, Q., Raza, A., Li, H., Sett, S., Miljkovic, N., and Zhang, T. (2020). Condensation of Satellite Droplets on Lubricant-Cloaked Droplets. ACS Appl. Mater. Interfaces 12, 22246–22255.
- Bjelobrk, N., Girard, H.-L., Subramanyam, S.B., Kwon, H.-M., Quéré, D., and Varanasi, K.K. (2016). Thermocapillary motion on lubricantimpregnated surfaces. Phys. Rev. Fluids 1, 063902.
- Miljkovic, N., Enright, R., and Wang, E.N. (2013). Modeling and optimization of superhydrophobic condensation. J. Heat Transfer 135, 111004.
- Sirohia, G.K., and Dai, X. (2019). Designing airindependent slippery rough surfaces for condensation. Int. J. Heat Mass Transf. 140, 777-785.
- 32. Vella, D., and Mahadevan, L. (2005). The "Cheerios effect". Am. J. Physiol. 73, 817–825.
- Kralchevsky, P.A., Paunov, V.N., Ivanov, I.B., and Nagayama, K. (1992). Capillary meniscus interaction between colloidal particles attached to a liquid—fluid interface. J. Colloid Interface Sci. 151, 79–94.
- 34. Kralchevsky, P.A., Paunov, V.N., Denkov, N.D., and Nagayama, K. (1994). Capillary Image Forces: I. Theory. J. Colloid Interface Sci. *167*, 47–65.
- Paunov, V.N., Kralchevsky, P.A., Denkov, N.D., and Nagayama, K. (1993). Lateral Capillary Forces between Floating Submillimeter Particles. J. Colloid Interface Sci. 157, 100–112.
- Landau, L., and Levich, B. (1988). Dragging of a liquid by a moving plate. Dyn. Curved Fronts, 141–153
- Daniel, D., Timonen, J.V., Li, R., Velling, S.J., and Aizenberg, J. (2017). Oleoplaning droplets on lubricated surfaces. Nat. Phys. 13, 1020– 1025.
- Stone, H.A., and Leal, L. (1990). Breakup of concentric double emulsion droplets in linear flows. J. Fluid Mech. 211, 123–156.